MC-PWM Harmonic Losses Determination in IPMSM drive fed by Cascaded H-Bridges Multilevel Inverter

Antonino Oscar Di Tommaso
Department of Engineering
University of Palermo
Palermo, Italy
antoninooscar.ditommaso@unipa.it

Rosario Miceli
Department of Engineering
line 3: *University of Palermo*
Palermo, Italy
rosario.miceli@unipa.it

Claudio Nevoloso
Department of Engineering
University of Palermo
Palermo, Italy
claudio.nevoloso@unipa.it

Gioacchino Scaglione
Department of Engineering
University of Palermo
Palermo, Italy
gioacchino.scaglione@unipa.it

Giuseppe Schettino
Department of Engineering
University of Palermo
Palermo, Italy
giuseppe.schettino@unipa.it

Ciro Spataro
Department of Engineering
University of Palermo
Palermo, Italy
ciro.spataro@unipa.it

***Abstract*— The use of Multilevel Inverters (MIs) in PMSM drives is a possible solution for motor harmonic power losses reduction. In this regard, their experimental determination is a challenging task. This paper addresses an experimental analysis of harmonic losses introduced in an IPMSM drive fed by a Cascaded H-Bridges Multilevel Inverter (CHBMI) controlled with different MultiCarrier PWM strategies (MC-PWM). For this purpose, a frequency domain power analysis approach has been adopted to separate the active power value generated at the fundamental harmonic frequency and the power losses at the higher harmonics. In this analysis, several working conditions, defined in the frequency-torque plane, have been considered and the detected IPMSM total power losses, fundamental power losses and harmonic power losses have been discussed.**

Keywords*— *PMSM, CHBMI, power measurement, power losses, harmonic power losses.

I. INTRODUCTION

Electric drives are the largest electricity-consumers and a further increase in electrical energy consumption is expected in the future due to the electrification of transportation systems, and the development of more automotive and industrial electric drives [1]. In this scenario, the majority of adjustable-speed drives are fed by two-level Voltage Source Inverters (VSIs), that allow to obtain several benefits such as motor soft-starting capabilities, partial load operations with energy-saving benefits and torque and speed control [2]. Generally, the conventional VSIs are controlled with the Pulse-Width Modulation (PWM) which presents several benefits but introduces additional power losses compared to sinusoidal grid supply, which reduces the motor efficiency, and thus, the drive efficiency [3]-[4]. These additional power losses are named harmonic power losses.

In this context, the scientific and industrial communities perform several efforts to improve electric drive performances and to reduce motor power losses by control algorithms, hardware solutions and with the release of new standardization bodies [5]-[6]. In detail, the last ones define new energy efficiency classification for motors, Complete Drive Modules (CDMs) and Power Drive Systems (PDSs) for energy savings purposes. Furthermore, a possible solution for motor power losses reduction is the use of Multilevel Inverters (MIs). In recent years, Cascaded H-Bridges Multilevel Inverters (MIs) have gained considerable interest in industrial medium voltage drives [8]-[9] due to their modular structure, lower total harmonics distortion (THD), higher efficiency, increased voltage/power-handling capability and fault-tolerant capability [10]. Furthermore, CHBMI drives are a fascinating solution in traction applications, especially in automotive, due to the easy integration with battery packs and an increase of the total DC link voltage, in accordance with actual industry trend [11]-[12]. With respect to conventional two-level inverters, the use of CHBMIs in electric drives guarantees a reduction of motor power harmonic losses and, thus, its accurate experimental determination is a challenging task.

The phenomenon of additional harmonic power losses in electrical machines fed by VSIs is a widespread and discussed topic in the literature. Although several works in literature address their mathematical and numerical modelling for motor control purposes [13], harmonic losses experimental assessment is a challenging task. The direct harmonic losses determination in induction motor drives is well-known and, generally, the Segregation Losses (SL) approach is used or they are determined as the difference between the total electric powers measured with PWM supply and sinusoidal one [14]. The SL approach can be applied also to PMSM drives, but it is very time-consuming. Furthermore, it is not guaranteed that the motor fed with different supplies presents the same temperature and magnetic working conditions for fixed load operation. An interesting measurement approach is proposed in [15], but it requires the accurate determination of magnetic quantities. The overwhelming majority of the studies proposed in literature focus on PMSM drives fed by conventional two-level VSI controlled with PWM strategy and it is necessary to consider that the motor harmonics losses depend on motor load conditions, adopted modulation strategy and switching frequency. Since MIs harmonic behaviour strongly depends on the adopted MC-PWM strategy, the investigation of PMSM behaviour in terms of harmonic losses is crucial.

This paper proposes a procedure for the experimental determination of harmonic losses in an IPMSM drive fed by CHBMI controlled with MC-PWM strategies and the results

obtained are discussed. In this regard, the frequency domain power analysis approach is used [16] and the total power losses, fundamental power losses and harmonics power losses have been determined for different IPMSM working conditions. The CHBMI is controlled with Switching Frequency Optimal Phase Shifted (SFOPS) and Switching Frequency Optimal Phase Disposition (SFOPD) MC-PWM strategies that present different voltage harmonic behaviour. The paper is structured as follows: Section II presents the harmonics power analysis for the determination of harmonic power losses; Section III presents the test bench for accurate measurement of electrical and mechanical quantities; Section IV presents the experimental investigations and discusses the obtained results. Finally, section VI summarizes the analysis and results of this work.

II. Harmonic Power Analysis

Generally, the electrical active power is experimentally determined from the sampled voltage and current signals with the equation:

$$P_{el} = \frac{1}{N_s}\sum_{k=0}^{N_s-1} v_k i_k \tag{1}$$

where N_s is the total number of acquired samples and v_k and i_k represent the instantaneous voltage and current samples. Similarly, the electrical active power can be obtained by applying the Discrete Fourier Transform (DFT). In detail, the total input power can be calculated by the following expression:

$$P_{el} = P_{DC} + \sum_{h=1}^{\infty} V_h I_h \cos(\varphi_h) \tag{2}$$

where P_{DC} is the DC power, V_h and I_h are the RMS values of h-order harmonic and φ_h is the respective phase displacement. In detail, the active power is generated by only isofrequential voltage and current harmonics and this approach includes all harmonic components: subharmonic and interharmonic components. Thus, by determining with this approach the total active power absorbed by each phase, the total active input power of a three-phase electrical motor can be calculated as:

$$P_{in} = P_{inA} + P_{inB} + P_{inC} \tag{3}$$

Moreover, the total active power can be expressed as the sum of fundamental power P_{h1}, determined by considering fundamental voltage and current quantities amplitude and their phase displacement, and harmonic power P_{harm} as:

$$P_{in} = P_{h1} + P_{harm} \tag{4}$$

By assuming that the high-frequency harmonics quantities have negligible impact on the torque production, the total power losses, the relative fundamental power losses and harmonic power losses can be determined with the following equations:

$$\Delta P_{tot} = P_{in} - P_m \tag{5}$$

$$\Delta P_1 = P_{h1} - P_m \tag{6}$$

$$\Delta P_{harm} = P_{harm} = \Delta P_{tot} - \Delta P_1 = P_{in} - P_{h1} \tag{7}$$

where P_m is the motor output power or the mechanical power. Furthermore, the power loss quantities can be expressed in percentage value as follows:

$$\Delta P_1[\%] = \frac{\Delta P_1}{\Delta P_{tot}} 100 \tag{8}$$

$$\Delta P_{harm}[\%] = \frac{\Delta P_{harm}}{\Delta P_{tot}} 100 \tag{9}$$

In this analysis, particular attention has to be paid to the determination of fundamental quantities and, therefore, it is necessary to consider the leakage spectrum phenomenon and set the observation time to obtain an appropriate frequency resolution. In this work, the observation time and relative sampling frequency have been set equal to 1 s and 1 MHz, respectively, by obtaining a frequency resolution of 1 Hz and synchronous sampling that results in the acquisition of an integer number of current and voltage waveform periods. Therefore, the leakage spectrum phenomenon is negligible.

III. Test Set Up

The proposed analysis has been performed on a three-phase IPMSM prototype fed by a three-phase five-level MOSFET-based CHBMI, whose circuit diagram is reported in Fig. 1 and the main technical data are reported in Table I. A test bench has been set up for accurate detection of harmonics power losses (Fig. 2) at SDESLab of the University of Palermo. The test bench is composed of a three-phase, six poles IPMSM with interior SmCo PMs, whose main data are reported in Table II and its main electrical and magnetic parameters are described and discussed in [17]. The CHBMI is powered by six DC power supply RSO-2400 whose datasheet is reported in [18].

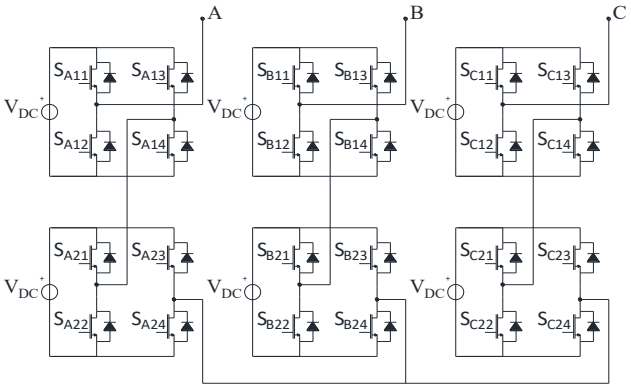

Fig. 1 CHBMI circuit diagram.

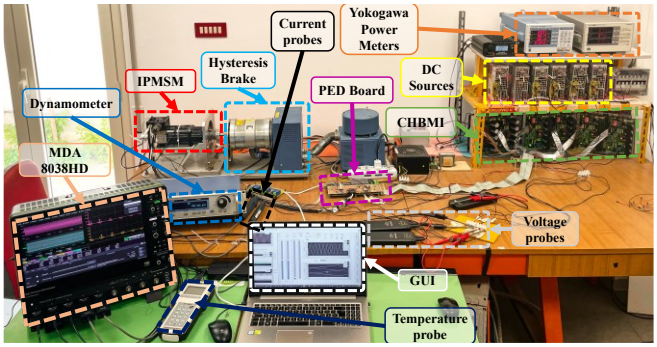

Fig. 2 Test bench.

TABLE I. CHBMI MOSFET-BASED-IRFB4115PBF DATA

Quantity	Symbol	Value
Voltage	V_{dss}	150 V
Resistance	R_{dSon}	9.3 mΩ
Current	I_D	104 A
Turn on delay	T_{Don}	18 ns
Rise time	T_R	73ns
Turn off delay	T_{Doff}	41 ns
Fall time	T_F	39ns
Reverse recovery	T_{RR}	86 ns

TABLE II. IPMSM RATED DATA.

Quantity	Symbol	Value
Rated Voltage	V_n	132 V
Rated current	I_n	3.6 A
Nominal Speed	n	4000 rpm
Maximum Speed	n_{max}	6000 rpm
Nr. of pole pairs	P	3
Nr. of phases	M	3
Nominal torque	T_{emn}	1.8 Nm
Peak torque	T_{emmax}	9.2 Nm

The accurate detection of IPMSM input active power is performed by a Teledyne LeCroy MDA 8038HD oscilloscope equipped with high-voltage differential probes Teledyne Lecroy HVD3106A, high sensitivity current probe Teledyne Lecroy CP030A and a deskew calibration source DCS025 for power angle error reduction. The manufacturer of measurement systems declares an accuracy A guaranteed of 1 % in the measured active power. By considering that the determination of harmonic power is only a function of electrical quantities (see equation 7), it is possible to assert the same accuracy for the determination of harmonic power or IPMSM harmonic power losses. Therefore, by considering a rectangular probability distribution, the standard uncertainty of electrical power $u(P_{in})$ and harmonic power $u(P_h)$ can be obtained with the follow expression:

$$u(P_{in}) = u(P_{harm}) = \frac{A}{\sqrt{2}} = 0.7\% \tag{10}$$

A Magtrol HD-715-8NA hysteresis brake is used to perform load tests and the relative dynamometer allows the measurement of IPMSM torque and speed with the consequent determination of mechanical power. The dynamometer provides torque and speed signals that have been acquired with MDA 8038HD oscilloscope. To detect the thermal equilibrium of IPMSM during load operations, a Delta Ohm temperature probe model DO 9847 has been employed.

The IPMSM drive is controlled by a Field Oriented Control (FOC) strategy, whose schematic diagram is reported in Fig. 3, implemented on a System on Module (SOM) sbRIO 9651 composed of an ARM Cortex-A9 processor and an Artix7 FPGA unit programmable in the Labview graphic language. This control strategy presents speed and currents closed-loop control performed by the use of digital PI controllers. The i_d current has been set equal to 0 A for simplicity and because flux weakening operations are not considered in this work. This choice is the optimal solution for comparison purposes. The peculiar feature of the FOC control consists in the possibility to vary the adopted modulation strategy and its switching frequency f_{sw}, as described in [19]. In this regard, the output voltages obtained by the FOC are modulated with two different MC-PWM modulation strategies. In detail, the MC-PWM strategies considered are obtained by combining PD and PS modulation schemes with Switching Frequency Optimal (SFO) modulation signals, whose modulation schemes are reported in Fig. 4 (a)-(b). These modulation schemes are the most suitable for electric drive applications [11] and the use of SFO modulation signals allows to extend the linear variation of the modulation index in the same way as Space Vector Modulation (SVM). The two modulation strategies present different harmonic behaviour. In detail, SFOPD modulation presents voltage harmonics centered at the switching frequency and its integer multiples, whereas SFOPS modulation presents harmonics centered at four times of the switching frequency and integer multiples [20]. In this analysis, the switching frequency f_{sw} has been set equal to 4 kHz.

In order to perform an extended experimental analysis, several IPMSM working conditions have been considered for a total of 16 Working Points (WPs). The IPMSM working points are defined for 25%, 50%, 75% and 100% of rated torque and by applying the supply fundamental frequency equal to 10 Hz, 50 Hz, 100 Hz and 150 Hz. The goal is to obtain an accurate loss mapping of total power losses, fundamental power losses and harmonic power losses. The IPMSM WPs considered for experimental analysis are reported in Fig. 5 as a function of the correspective IPMSM speed. All the experimental investigations have been carried out with IPMSM at thermal equilibrium.

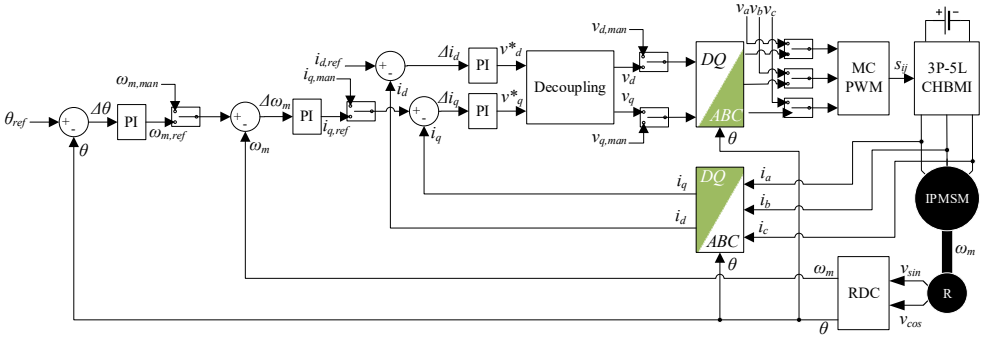

Fig. 3 FOC schematic diagram.

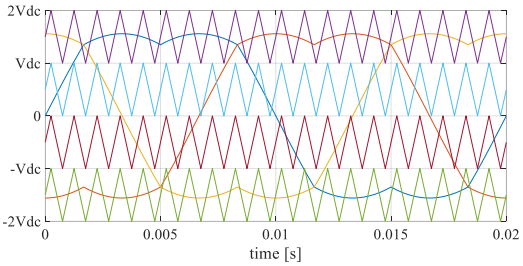

(a)

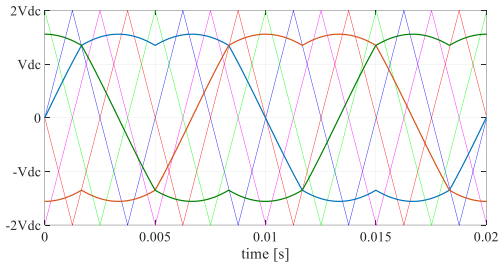

(b)

Fig. 4 MC-PWM strategies employed: (b) SFOPD, (c) SFOPS.

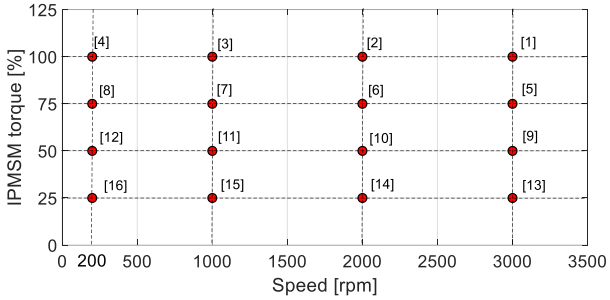

Fig. 5 IPMSM working points.

IV. Experimental Investigations and Analysis

The experimental investigations have been performed for the previously defined IPMSM working conditions, by controlling the CHBMI with SFOPS and SFOPD modulation strategies. Moreover, for each IPMSM WP, the measurement has been repeated three times for repeatability purposes. By considering that for each measurement point, three voltage and three current signals have been acquired with a sampling frequency equal to 1 MHz and a time window equal to 1 s, a huge amount of data have been acquired. The acquired data of all test points have been analyzed in Matlab® environment. No significant differences have been detected in power analysis for each repeated measurement and, thus, the results relative to the first acquisition for each IPMSM WP have been reported and discussed. By way of example, the IPMSM voltage and currents acquired ad WP 2 with SFOPD and SFOPS modulation strategies are shown in Fig. 6 (a) and Fig. 6 (b), respectively. Furthermore, by performing the DFT on voltages and currents, described in Section II, the IPMSM active power trend in the frequency domain has been obtained for each considered WP. By way of example, to appreciate the impact of voltage and current harmonics on IPMSM input active power in the frequency domain, the cumulative IPMSM active power detected at WP 2, expressed in percent value of total active power, is reported in Fig. 7 (a)-(b) for the two considered modulation strategies. In detail, it is possible to observe that more than 99.5 % of IPMSM active power is generated by fundamental quantities and it is possible to highlight a small step variation of its active power due to the third harmonic quantities in both modulation strategies. These results can be attributed both to the use of CHBMI to feed the IPMSM that introduces a reduced voltage harmonic content and to the non-linear magnetic behaviour of IPMSM that introduces a small third harmonic both in the motor and in the supply voltages, respectively.

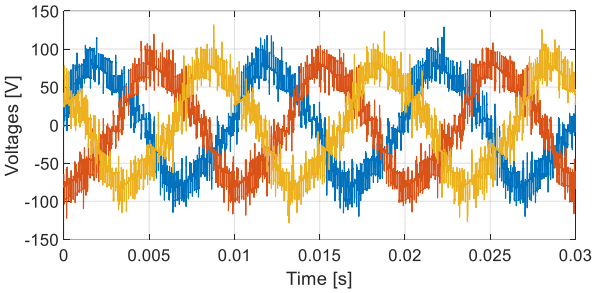

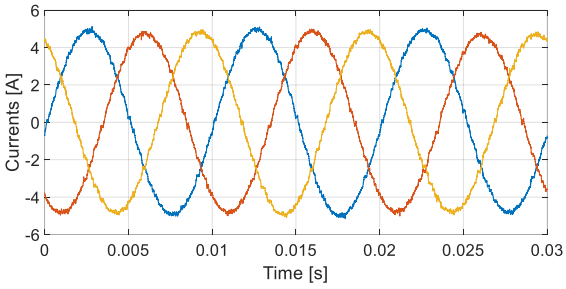

(a)

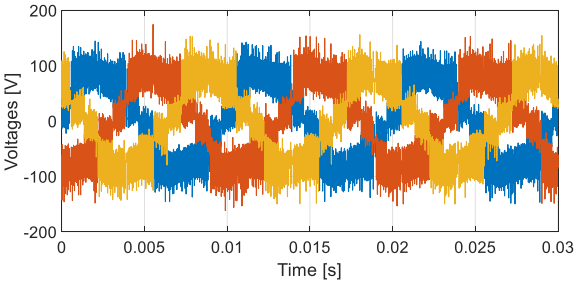

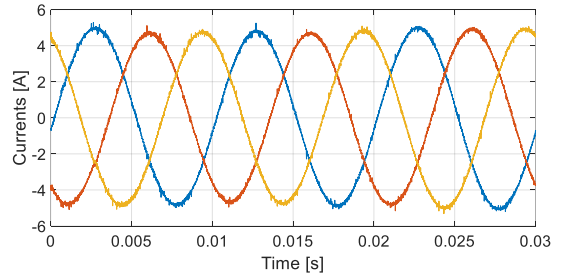

(b)

Fig. 6 IPMSM voltage and current quantities acquired at WP 2: (a) SFOPD, (b) SFOPS.

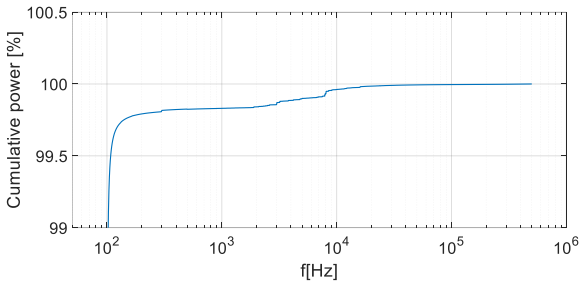

(a)

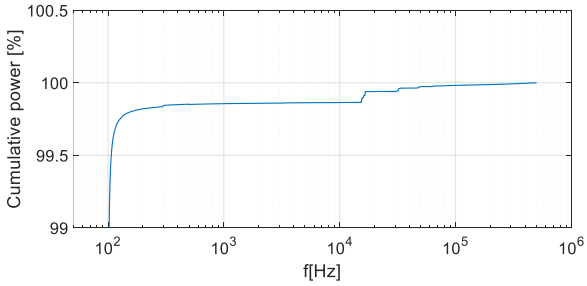

(b)

Fig. 7 Cumulative IPMSM input active power trend, expressed in percent value, as a function of the frequency: (a) SFOPD, (b) SFOPS.

Moreover, as expected, in the SFOPD modulation strategy a step variation of the IPMSM active power has been detected at 4 KHz and integer multiplies of it, whereas for SFOPS the same result has been detected at 16 kHz and integer multiplies of it. In both cases, the voltage and current harmonics operating at frequency values higher than 100 kHz present negligible impact in terms of active power. The IPMSM total power losses detected for all IPMSM WPs for each modulation strategy are summarized in loss maps depicted in Fig. 8 and Fig. 9, respectively. In detail, the IPMSM presents lower total power losses when the CHBMI is controlled with the SFOPD modulation strategy. This behaviour is more significant at high load torque values and the difference in terms of total power losses can be considered negligible for low values of load torque. Therefore, better IPMSM performances in terms of power losses are obtained when it is controlled with the SFOPD modulation strategy.

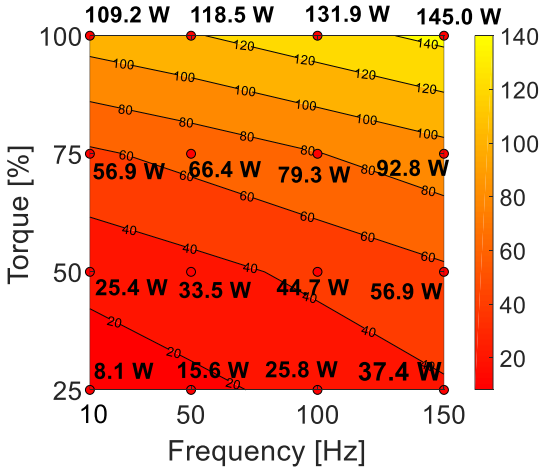

Fig. 8 IPMSM total power losses detected with SFOPD modulation strategy.

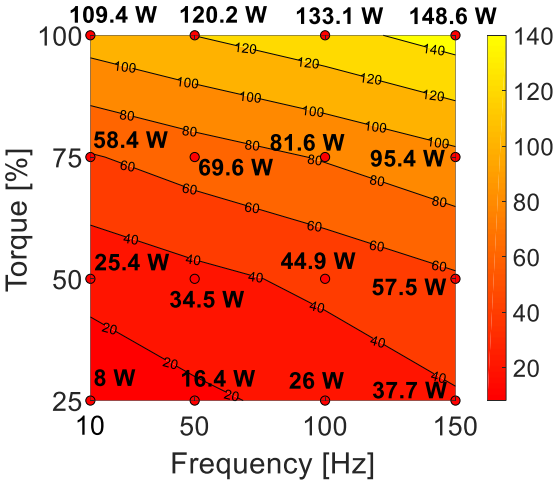

Fig. 9 IPMSM total power losses detected with SFOPS modulation strategy.

In order to perform a more accurate power losses analysis, the obtained IPMSM total power losses are decomposed into fundamental and harmonic power losses by applying the described DFT approach reported in section II. In detail, the IPMSM fundamental and harmonic power losses obtained with the two mentioned modulation strategies are reported in Fig. 10 and Fig. 11, respectively.

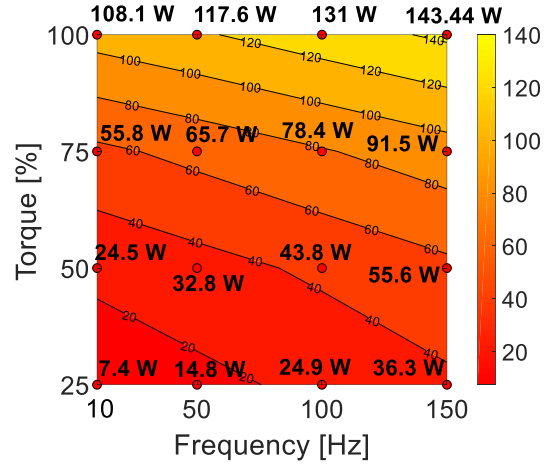

(a)

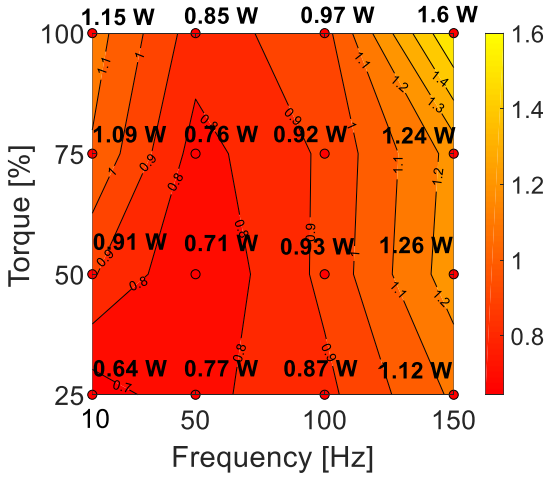

(b)

Fig. 10 (a) IPMSM fundamental power losses and (b) IPMSM harmonic power losses detected with SFOPD modulation strategy.

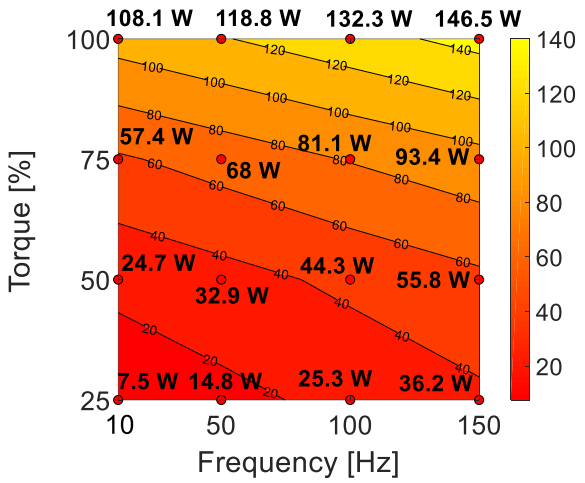

(a)

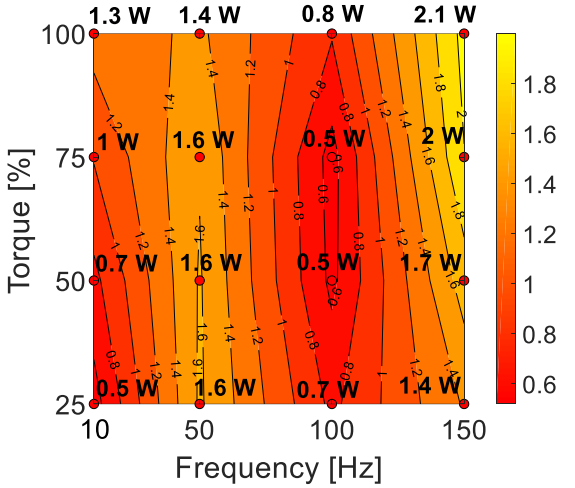

(b)

Fig. 11 (a) IPMSM fundamental power losses and (b) IPMSM harmonic power losses detected with SFOPS modulation strategy.

The results obtained show that the differences in terms of fundamental power losses are appreciable at high load torque and negligible at low values of load torque. Contrariwise, higher harmonic power losses have been detected during the SFOPS modulation strategy. This behaviour can be attributed to the higher voltage frequency harmonic components introduced by the SFOPS modulation strategy that can be associated with respective higher frequency flux harmonic components in the motor, which are sources of additional iron losses. In this analysis, it is necessary to consider that the inductive behaviour of IPMSM filters the high-frequency current harmonic component and, thus, the associated copper losses can be considered negligible. Furthermore, the IPMSM fundamental power losses and harmonic power losses expressed in percentage values are reported in Fig. 12 (a-b) and Fig. 13 (a-b) for the two modulation strategies considered, respectively. It is possible to observe that the IPMSM fundamental power losses are higher than 90% in all IPMSM WPs in both modulation strategies. Moreover, the IPMSM fundamental power losses percentage values decrease as the torque load decreases and the lowest values have been detected at WPs 16 where the lowest fundamental frequency is employed. Appreciable variations of IPMSM fundamental power losses percentage values as a function of supply frequency have been detected only for the lowest value of load torque in both modulation strategies.

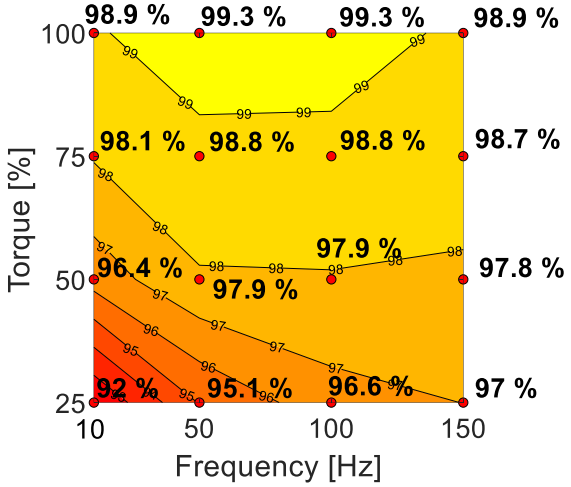

(a)

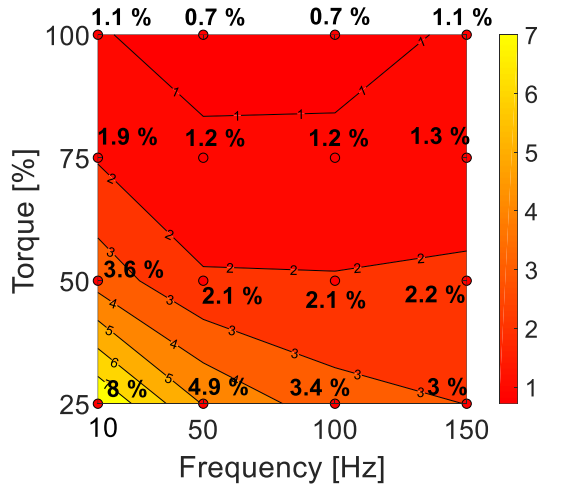

(b)

Fig. 12 (a) IPMSM percentage fundamental power losses and (b) IPMSM percentage harmonic power losses detected with SFOPD modulation strategy.

For comparison purposes, it is possible to highlight that the IPMSM presents higher harmonic power losses percentage values when the SFOPS modulation strategy is employed in almost all WPs. The analysis carried out shows that the vast majority of IPMSM power losses are generated by the fundamental electrical quantities in both modulation strategies but to a greater extent in the use of the SFOPD modulation strategy. The analysis conducted allows to perform several considerations for comparison purposes with IPMSM drives fed by conventional two-level VSIs. Since the typical IPMSM control algorithms are based on fundamental harmonic control, only the fundamental power losses are controllable and can be easily reduced. Therefore, the analysis carried out shows that the IPMSM presents very reduced harmonic power losses when it is supplied by CHBMI and further IPMSM power losses reduction can be obtained by optimal control of fundamental quantities. Although the impact of the harmonic power losses is a function of the IPMSM rated power, several works in literature show that significant harmonic power losses are obtained when conventional two-level VSIs, controlled with PWM strategy, are employed and their values vary from 5% up to 30% of the total losses [4],[21]. These

results allow to assert that the IPMSM drives fed by CHBMI present significant margins in terms of power losses reduction with respect to conventional two-level VSIs and these results are of relevant interest, especially in medium-high voltage applications.

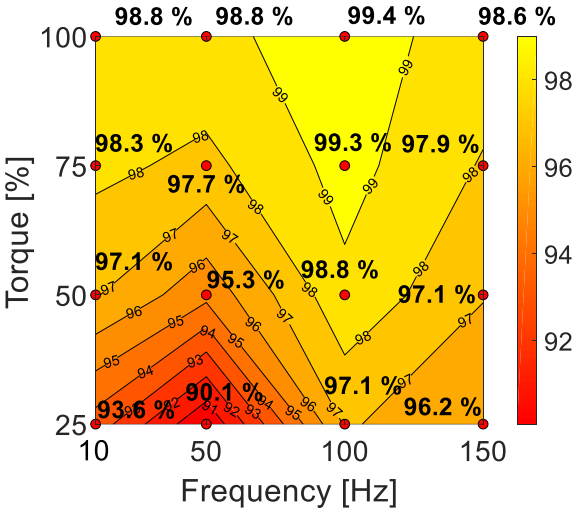

(a)

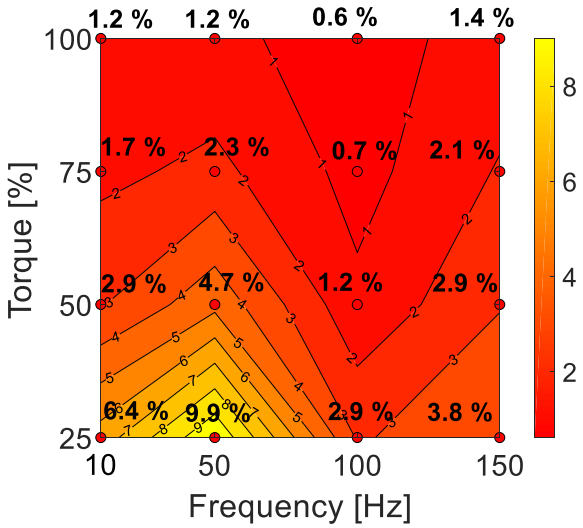

(b)

Fig. 13 (a) IPMSM percentage fundamental power losses and (b) IPMSM percentage harmonic power losses detected with SFOPS modulation strategy.

V. Conclusions

This work presents an experimental analysis of IPMSM performance in terms of power losses when it is supplied with a CHBMI controlled with two different MC-PWM strategies. In detail, the analysis employs the DFT approach to separate the total power losses into fundamental power losses and harmonic ones. Experimental tests have been carried out for sixteen different IPMSM working conditions defined in the torque-speed plane. The analysis conducted shows that the IPMSM presents higher power losses when the SFOPS modulation strategy is employed. This behaviour can be attributed to the SFOPS voltage harmonic spectrum placed at higher frequency values, with respect to those of SFOPD, that increase the IPMSM harmonic iron losses. Furthermore, the power losses analysis performed in terms of fundamental power losses and harmonic power losses, expressed in percentage values, highlighted that the IPSMS harmonic losses present very low values in both modulation strategies. Since the main source of power losses in power drive systems is the motor and its power losses generated by fundamental quantity are controllable, significant margins of IPMSM efficiency improvement can be obtained with the use of CHBMIs instead of conventional two-level VSIs.

Acknowledgment

This work was supported in part by the Prin 2017-Settore/Ambito di intervento: PE7 linea C Advanced power-trains and -systems for full electric aircrafts under Grant 2017MS9F49 and in part by the Sustainable Mobility Center (Centro Nazionale per la Mobilità Sostenibile—CNMS) under Grant CN00000023 CUP B73C22000760001.

References

[1] L. Aarniovuori, H. Kärkkäinen, A. Anuchin, J. J. Pyrhönen, P. Lindh and W. Cao, "Voltage-Source Converter Energy Efficiency Classification in Accordance With IEC 61800-9-2," in *IEEE Transactions on Industrial Electronics*, vol. 67, no. 10, pp. 8242-8251, Oct. 2020.

[2] H. Karkkainen, L. Aarniovuori, M. Niemela and J. Pyrhonen, "Converter-Fed Induction Motor Efficiency: Practical Applicability of IEC Methods," in *IEEE Industrial Electronics Magazine*, vol. 11, no. 2, pp. 45-57, June 2017.

[3] L. Aarniovuori, H. Kärkkäinen, M. Niemelä, K. Cai, J. Pyrhönen and W. Cao, "Experimental Investigation of the Losses and Efficiency of 75 kW Induction Motor Drive System," IECON 2019 - 45th Annual Conference of the *IEEE Industrial Electronics Society*, Lisbon, Portugal, 2019, pp. 1052-1058.

[4] Y. Miyama, M. Hazeyama, S. Hanioka, N. Watanabe, A. Daikoku and M. Inoue, "PWM carrier harmonic iron loss reduction technique of permanent magnet motors for electric vehicles," 2015 IEEE International Electric Machines & Drives Conference (IEMDC), Coeur d'Alene, ID, USA, 2015, pp. 475-481.

[5] IEC 61800-9-1. Adjustable speed electrical power drive systems - Part 9-1: Ecodesign for power drive systems, motor starters, power electronics and their driven applications - General requirements for setting energy efficiency standards for power driven equipment using the extended product approach (EPA) and semi analytic model (SAM), 2017.

[6] IEC 61800-9-2. Adjustable Speed Electrical Power Drive Systems—Part 9-2: Ecodesign for Power Drive Systems, Motor Starters, Power Electronics & Their Driven Applications—Energy Efficiency Indicators for Power Drive Systems and Motor Starters, 2017.

[7] L. Liu, H. Li, S. -H. Hwang and J. -M. Kim, "An Energy-Efficient Motor Drive With Autonomous Power Regenerative Control System Based on Cascaded Multilevel Inverters and Segmented Energy Storage," in *IEEE Transactions on Industry Applications*, vol. 49, no. 1, pp. 178-188, Jan.-Feb. 2013.

[8] A. Marzoughi, R. Burgos and D. Boroyevich, "Investigating Impact of Emerging Medium-Voltage SiC MOSFETs on Medium-Voltage High-Power Industrial Motor Drives," in *IEEE Journal of Emerging and Selected Topics in Power Electronics*, vol. 7, no. 2, pp. 1371-1387, June 2019.

[9] H. Abu-Rub, J. Holtz, J. Rodriguez and G. Baoming, "Medium-Voltage Multilevel Converters—State of the Art, Challenges, and Requirements in Industrial Applications," in *IEEE Transactions on Industrial Electronics*, vol. 57, no. 8, pp. 2581-2596, Aug. 2010.

[10] C. Buccella et al., "Recursive Selective Harmonic Elimination for Multilevel Inverters: Mathematical Formulation and Experimental Validation," in *IEEE Journal of Emerging and Selected Topics in Power Electronics*, vol. 11, no. 2, pp. 2178-2189, April 2023.

[11] A. Poorfakhraei, M. Narimani and A. Emadi, "A Review of Modulation and Control Techniques for Multilevel Inverters in Traction Applications," in IEEE Access, vol. 9, pp. 24187-24204, 2021.

[12] F. Chang, O. Ilina, M. Lienkamp and L. Voss, "Improving the Overall Efficiency of Automotive Inverters Using a Multilevel Converter Composed of Low Voltage Si mosfets," in *IEEE Transactions on Power Electronics*, vol. 34, no. 4, pp. 3586-3602, April 2019.

[13] A. Balamurali, A. Kundu, Z. Li and N. C. Kar, "Improved Harmonic Iron Loss and Stator Current Vector Determination for Maximum Efficiency Control of PMSM in EV Applications," in *IEEE Transactions on Industry Applications*, vol. 57, no. 1, pp. 363-373, Jan.-Feb. 2021.

[14] E. B. Agamloh, A. Cavagnino and S. Vaschetto, "Standard Efficiency Determination of Induction Motors With a PWM Inverter Source," in *IEEE Transactions on Industry Applications*, vol. 55, no. 1, pp. 398-406, Jan.-Feb. 2019.

[15] J. Richter, A. Dollinger and M. Doppelbauer, "Iron loss and parameter measurement of permanent magnet synchronous machines," 2014 International Conference on Electrical Machines (ICEM), Berlin, Germany, 2014, pp. 1635-1641.

[16] L. Aarniovuori, H. Kärkkäinen, M. Niemelä and J. Pyrhönen, "PWM-Induced Harmonic Power in 75 kW IM Drive System," 2020 22nd European Conference on Power Electronics and Applications (EPE'20 ECCE Europe), Lyon, France, 2020, pp. P.1-P.9.

[17] M. Caruso, A.O. Di Tommaso, R. Miceli, C. Nevoloso, C. Spataro, F. Viola, Characterization of the parameters of interior permanent magnet synchronous motors for a loss model algorithm, *Measurement*, Volume 106, 2017, Pages 196-202, ISSN 0263-2241.

[18] https://www.meanwell.com/Upload/PDF/RSP-2400/RSP-2400-SPEC.PDF.

[19] A. O. D. Tommaso et al., "Field Oriented Control of IPMSM Fed by Multilevel Cascaded H-Bridges Inverter with NI-SOM sbRIO-9651 FPGA controller," 2022 International Symposium on Power Electronics, Electrical Drives, Automation and Motion (SPEEDAM), Sorrento, Italy, 2022, pp. 88-93.

[20] Busacca, A.; Di Tommaso, A.O.; Miceli, R.; Nevoloso, C.; Schettino, G.; Scaglione, G.; Viola, F.; Colak, I. Switching Frequency Effects on the Efficiency and Harmonic Distortion in a Three-Phase Five-Level CHBMI Prototype with Multicarrier PWM Schemes: Experimental Analysis. Energies 2022, 15, 586.

[21] J. Heseding, F. Mueller-Deile and A. Mertens, "Estimation of losses in permanent magnet synchronous machines caused by inverter voltage harmonics in driving cycle operation," 2016 18th European Conference on Power Electronics and Applications (EPE'16 ECCE Europe), Karlsruhe, Germany, 2016, pp. 1-9.